ORAI1-mediated calcium influx is required for human cytotoxic lymphocyte degranulation and target cell lysis

Andrea Maul-Pavicic[a,1], Samuel C. C. Chiang[b,1], Anne Rensing-Ehl[a], Birthe Jessen[a], Cyril Fauriat[b], Stephanie M. Wood[b], Sebastian Sjöqvist[b], Markus Hufnagel[c], Ilka Schulze[a,c], Thilo Bass[d], Wolfgang W. Schamel[d], Sebastian Fuchs[a], Hanspeter Pircher[e], Christie-Ann McCarl[f], Katsuhiko Mikoshiba[g], Klaus Schwarz[a,h], Stefan Feske[f], Yenan T. Bryceson[b,2,3], and Stephan Ehl[a,c,2,3]

[a]Centre of Chronic Immunodeficiency and [c]Centre for Pediatrics and Adolescent Medicine, University Medical Center Freiburg, 79106 Freiburg, Germany; [b]Center for Infectious Medicine, Karolinska Institutet, 14186 Stockholm, Sweden; [d]Max Planck Institute for Immunobiology and Faculty of Biology, Institute for Biology III, and [e]Institute of Medical Microbiology and Hygiene, University of Freiburg, 79106 Freiburg, Germany; [f]Langone Medical Center, New York University, New York, NY 10016; [g]RIKEN Brain Science Institute, Wako City, Saitama 351-0198, Japan; and [h]Institute of Transfusion Medicine, University of Ulm, and Institute of Clinical Transfusion Medicine and Immunogenetics, 89081 Ulm, Germany

Edited by Wayne M. Yokoyama, Washington University School of Medicine, St. Louis, MO, and approved January 12, 2011 (received for review September 8, 2010)

Lymphocytes mediate cytotoxicity by polarized release of the contents of cytotoxic granules toward their target cells. Here, we have studied the role of the calcium release-activated calcium channel ORAI1 in human lymphocyte cytotoxicity. Natural killer (NK) cells obtained from an ORAI1-deficient patient displayed defective store-operated Ca^{2+} entry (SOCE) and severely defective cytotoxic granule exocytosis leading to impaired target cell lysis. Similar findings were obtained using NK cells from a stromal interaction molecule 1-deficient patient. The defect occurred at a late stage of the signaling process, because activation of leukocyte functional antigen (LFA)-1 and cytotoxic granule polarization were not impaired. Moreover, pharmacological inhibition of SOCE interfered with degranulation and target cell lysis by freshly isolated NK cells and $CD8^+$ effector T cells from healthy donors. In addition to effects on lymphocyte cytotoxicity, synthesis of the chemokine macrophage inflammatory protein-1β and the cytokines TNF-α and IFN-γ on target cell recognition was impaired in ORAI1-deficient NK cells, as previously described for T cells. By contrast, NK cell cytokine production induced by combinations of IL-12, IL-15, and IL-18 was not impaired by ORAI1 deficiency. Taken together, these results identify a critical role for ORAI1-mediated Ca^{2+} influx in granule exocytosis for lymphocyte cytotoxicity as well as for cytokine production induced by target cell recognition.

primary immunodeficiency | cytotoxic lymphocytes | lytic granules | perforin

Cytotoxic lymphocytes, such as $CD8^+$ T cells and natural killer (NK) cells, can kill virus-infected or transformed cells through polarized release of the contents of cytotoxic granules (1, 2). On recognition of target cells via the T-cell receptor or activating NK cell receptors, cytotoxic granules are anchored to microtubules and migrate toward the immune synapse, together with the microtubule organizing center (MTOC) (3, 4). Polarized cytotoxic granules fuse with the cell membrane, leading to release of the granule content into the synaptic cleft. The pore-forming protein perforin then provides granzymes access to target cells, where they induce apoptotic cell death (5).

Uptake of extracellular Ca^{2+} is required for lymphocyte cytotoxicity (6–8). Vesicle exocytosis in a cytotoxic T-cell [cytotoxic T-lymphocyte (CTL)] line has been described to require a Ca^{2+} current with calcium release-activated calcium (CRAC) channel characteristics (9). The nature of the Ca^{2+} channel that mediates Ca^{2+} influx and cytolytic function in cytotoxic lymphocytes has not been determined (2, 10). Moreover, the involvement of Ca^{2+} influx in signaling processes mediating target cell adhesion, cytolytic granule polarization, and exocytosis is not clear. In a remarkable series of experiments, ORAI1 and stromal interaction molecule 1 (STIM1) were identified as the molecular constituents of the CRAC channel in T cells (11–14). STIM1, localized in the endoplasmic reticulum (ER), acts as the sensor of Ca^{2+} depletion from the ER, and its physical interaction with ORAI1 triggers the opening of CRAC channels and influx of extracellular Ca^{2+}, a process termed store-operated Ca^{2+} entry (SOCE) (15). The key role of this pathway in immune cell function is illustrated by the severe immunodeficiency in patients with impaired CRAC channel function attributable to mutations in *ORAI1* and *STIM1* (13, 16, 17). Ca^{2+} influx is required for the activation of the transcription factor nuclear factor of activated T cells (NFAT), which, in turn, is essential for the expression of cytokines, such as IL-2. This pathway is defective in T cells from ORAI1-deficient patients (18).

Here, we have used NK cells from two patients who are ORAI1-deficient or STIM1-deficient, respectively, as well as CTLs and NK cells from healthy donors treated with inhibitors of SOCE to study the role of ORAI1 in lymphocyte cytotoxicity. Our results demonstrate that SOCE mediated via ORAI1 is critical for target cell-induced lytic granule exocytosis in NK cells and CTLs as well as for target cell-induced proinflammatory chemokine and cytokine production by human NK cells.

Results

ORAI1-Deficient NK Cells Show Defective SOCE. During reevaluation of a 15-y-old ORAI1-deficient patient (19) who had received a hematopoietic stem cell transplant at the age of 4 mo, cell-specific chimerism was determined. A short tandem repeat (STR) analysis was performed at 15 loci using DNA from whole blood from donor and recipient before transplantation and from sorted NK-, B-, and T-cell populations posttransplantation (Fig. 1*A*). After transplantation, the pattern of STRs in NK cells showed exclusively recipient signals, whereas there was a small donor signal among B and T cells (Fig. 1*B*). This indicates a mixed chimerism in the patient with a maximum of about

Author contributions: A.M.-P., S.C.C.C., K.S., S. Feske, Y.T.B., and S.E. designed research; A.M.-P., S.C.C.C., A.R.-E., B.J., C.F., S.M.W., S.S., T.B., W.W.S., and Y.T.B. performed research; M.H., I.S., S. Fuchs, H.P., C.-A.M., and K.M. contributed new reagents/analytic tools; A.M.-P., S.C.C.C., A.R.-E., B.J., C.F., S.M.W., S.S., T.B., W.W.S., K.S., S. Feske, Y.T.B., and S.E. analyzed data; and A.M.-P., S.C.C.C., S. Feske, Y.T.B., and S.E. wrote the paper.

The authors declare no conflict of interest.

This article is a PNAS Direct Submission.

[1]A.M.-P. and S.C.C.C. contributed equally to this work.

[2]Y.T.B. and S.E. contributed equally to this work.

[3]To whom correspondence may be addressed. E-mail: yenan.bryceson@ki.se or stephan.ehl@uniklinik-freiburg.de.

This article contains supporting information online at www.pnas.org/lookup/suppl/doi:10.1073/pnas.1013285108/-/DCSupplemental.

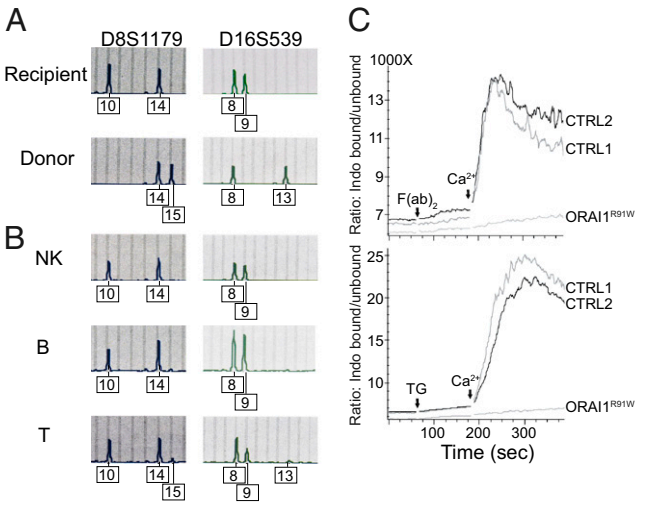

Fig. 1. ORAI1-deficient NK cells have impaired SOCE influx. (*A*) Split chimerism of lymphocyte subpopulations. STR analysis was performed at the indicated markers using DNA isolated from PBMCs of the patient (recipient) and the bone marrow donor before transplantation (*A*) and DNA isolated from the indicated purified cell populations after transplantation (*B*). Although there is a small donor signal (15 in locus 1 and 13 in locus 2) among T cells and a minimal donor signal among B cells, all NK cells are of recipient origin. (*C*) Ca^{2+} influx in stimulated NK cells. Purified NK cells from the patient (ORAI1^{R91W}) and two healthy donors (CRTL) were either preincubated with anti-CD16 mAb in Ca^{2+}-free PBS, followed by cross-linking and the addition of 2 mM $CaCl_2$ (*Upper*), or incubated with 1 μM TG, followed by the addition of 2 mM $CaCl_2$ (*Lower*). The graph shows the ratio of unbound to bound indo-1-AM as a measure of Ca^{2+} influx during the course of the experiment. The assay was performed twice with similar results. CTRL, control; TG, thapsigargin.

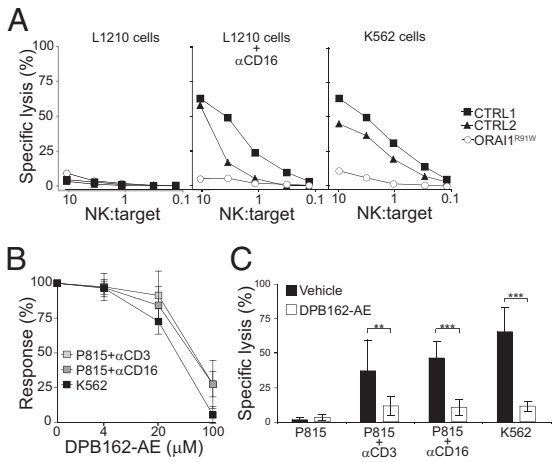

Fig. 2. ORAI1 dependence of lymphocyte cytotoxicity. (*A*) Cytotoxicity was assessed in a ^{51}Cr release assay using purified NK cells from the ORAI1-deficient patient (ORAI1^{R91W}) and two healthy donors (CTRL) as effector cells and target cells at the indicated effector/target (NK:target) ratios. For antibody-dependent cellular cytotoxicity, L1210 target cells were either preincubated with anti-CD16 mAb or left unlabeled. For natural cytotoxicity, K562 cells were used as target cells. CTRL, control. (*B* and *C*) PBMCs were preincubated with different concentrations of DPB162-AE, as indicated, for 30 min and mixed with ^{51}Cr-labeled K562 or P815 target cells as indicated. Specific lysis was assessed with an effector/target ratio of 100:1. Results are representative of four independent experiments. (*B*) Graph depicts the response calculated as the percentage of the specific lysis with different concentrations of DPB162-AE relative to that with vehicle only. Values with error bars represent mean ± SD of five donors. (*C*) Plots depict specific lysis with or without 100 μM DPB162-AE. Values with error bars represent mean ± SD of nine donors. Results are representative of at least three independent experiments. $^{**}P < 0.01$; $^{***}P < 0.001$.

10–15% donor T cells and 5% donor B cells, whereas all his NK cells were of host origin carrying the R91W single amino acid substitution in ORAI1 (Fig. 1*B*) (13). To analyze the consequences of this mutation for SOCE in NK cells, changes in intracellular Ca^{2+} levels were measured in purified NK cells following the passive depletion of intracellular Ca^{2+} stores. For this purpose, we either treated NK cells with thapsigargin (Fig. 1*C*, *Lower*), which depletes ER Ca^{2+} stores through inhibition of the sarco/endoplasmatic Ca^{2+} ATPase, or activated NK cells through cross-linking of CD16 (Fig. 1*C*, *Upper*), which causes emptying of ER Ca^{2+} stores via phospholipase C-γ activation and phosphoinositide generation. Freshly isolated NK cells were treated with thapsigargin or anti-CD16 mAb in the absence of extracellular Ca^{2+} (Fig. 1*C*). Readdition of Ca^{2+} to the medium led to robust Ca^{2+} influx in NK cells from healthy donors but not in NK cells from the patient, showing that ORAI1 is essential for SOCE in NK cells.

Notably, the ORAI1-deficient NK cells showed normal frequencies and expression levels of NK-cell activating and inhibitory receptors (Fig. S1), although it should be noted that the frequency of NK cells expressing the activating receptor CD2 and inhibitory receptor KLRG1 was unusually low on the patient's NK cells. ORAI1-deficient NK cells also displayed normal intracellular expression of perforin (Fig. S2).

Lymphocyte Cytotoxicity Is Dependent on ORAI1 and STIM1. Because uptake of extracellular Ca^{2+} is required for the cytolytic activity of CTLs, we next assessed cytotoxicity in ORAI1-deficient NK cells. Freshly purified ORAI1-deficient NK cells failed to lyse Fc receptor (FcR)-positive L1210 target cells after incubation with anti-CD16 mAbs and displayed severely impaired lysis of K562 cells (Fig. 2*A*), indicating defective antibody-dependent cellular cytotoxicity and natural cytotoxicity. We also studied NK cells from a 5-y-old STIM1-deficient patient carrying a R429C single amino acid substitution resulting in defective SOCE (Fig. S3). STIM1-deficient NK cells also displayed defective lysis of K562 target cells (Fig. S4).

To substantiate these data, we used pharmacological inhibitors of SOCE, DPB162-AE, and 2-APB (20, 21). DPB162-AE is a 2-APB analog recently characterized as a potent inhibitor of SOCE that disrupts puncta formation of STIM1, and thus activation of ORAI Ca^{2+} channels (21). DPB162-AE blocked SOCE in NK cells on readdition of extracellular Ca^{2+} after NK cells had been treated with thapsigargin or had been activated through cross-linking of CD16 (Fig. S5). DPB162-AE significantly inhibited NK cell-mediated lysis of K562 cells and CD16-dependent lysis of P815 cells in a dose-dependent manner (Fig. 2 *B* and *C*). DPB162-AE also inhibited T cell-mediated anti–CD3-dependent lysis of P815 cells (Fig. 2 *B* and *C*). Partial inhibition of K562 cell lysis was also observed with 100 μM 2-APB. At these concentrations, the pharmacological inhibitors were not cytotoxic (Fig. S6). Thus, pharmacological inhibition of SOCE abolished lymphocyte cytotoxicity induced by triggering of the T-cell receptor, the FcR CD16, and engagement of ligands for NK cell-mediated natural cytotoxicity.

Inside-Out Signals for LFA-1 Activation and Cytotoxic Granule Polarization Are Not Impaired by ORAI1 Deficiency. NK cell cytotoxicity comprises several steps, including target cell adhesion, granule polarization, and granule exocytosis (22, 23). Target cell adhesion through leukocyte functional antigen (LFA)-1 is augmented by so-called "inside-out signals," which lead to a conformational change in the ectodomain of LFA-1. Particular mAbs, such as 327C, specifically recognize this extended ligand-binding conformation of LFA-1 (24, 25). We assessed the role of ORAI1 in mediating these inside-out signals by stimulation of ORAI1-deficient CD56^{dim} NK cells with K562 cells or anti–CD16-coated P815 target cells. No defect in inside-out signals for LFA-1 activation was detected (Fig. 3*A*). Similar results were obtained using a series of previously described *Drosophila* Schneider 2 (S2)-cell

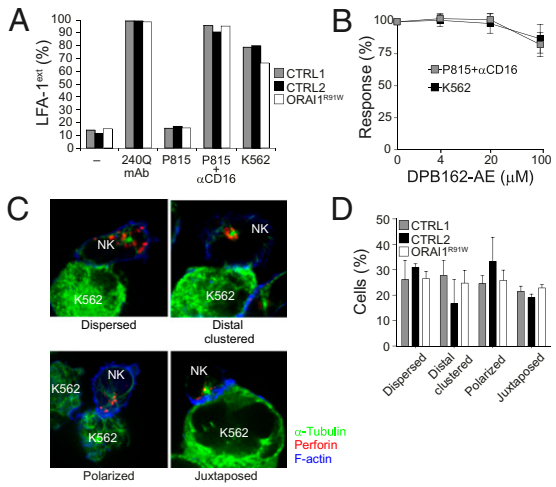

Fig. 3. Signals for LFA-1 activation and granule polarization are ORAI1-independent. (*A*) PBMCs from the ORAI1-deficient patient (ORAI1^{R91W}) or healthy donors (CTRL) were mixed with target cells as indicated. Cells were incubated for 5 min at 37 °C, stained with lineage marker and conformation-specific biotinylated anti–LFA-1 mAbs, washed, and stained with fluorochrome-conjugated streptavidin. The percentage of CD3$^-$ CD56^{dim} NK cells with 327C^{high} expression (LFA-1^{ext}), indicating LFA-1 in the extended ligand-binding conformation, is presented. One representative experiment of two is shown. (*B*) PBMCs from healthy donors were preincubated with different concentrations of DPB162-AE as indicated for 30 min, incubated with target cells, and stained as described in *A*. The graph depicts the response calculated as the percentage of 327C^{high} CD56^{dim} NK cells with varying concentrations of DPB162-AE relative to that with vehicle only. Values with error bars represent mean ± SD of four donors. (*C* and *D*) Purified NK cells from the ORAI1-deficient patient or healthy donors were mixed and incubated with K562 cells for 20 min, fixed, permeabilized, and stained intracellularly with phalloidin, α-tubulin, and perforin. Thereafter, NK cells in conjugates with target cells were scored for polarization of perforin granules and the MTOC. (*C*) Representative images of different categories of NK cell–K562 cell conjugates are shown. NK cells were derived from a healthy control. (*D*) Plot depicts the percentage of NK cells with different degrees of perforin granule and MTOC polarization, as indicated. Values with error bars represent mean ± SD of more than 190 conjugated NK cells derived from three independent experiments. CTRL, control.

transfectants expressing human intercellular adhesion molecule-1, CD48, ULBP1, or combinations thereof (25) (Fig. S7). Furthermore, in CD56^{dim} NK cells from healthy donors, the ORAI1 inhibitor DBP162-AE did not affect target cell-induced inside-out signals for LFA-1 activation (Fig. 3*B*).

To address the question of whether granule polarization is dependent on ORAI1, polarization of perforin-containing granules was analyzed in NK cells conjugated to K562 cells. Each NK cell–K562 cell conjugate was scored into one of the following categories: perforin granules and MTOC dispersed distally from target cell synapse (dispersed), perforin granules clustered distally at the MTOC (clustered distally), perforin granules and MTOC polarized toward the target cell synapse (polarized), or perforin granules and MTOC immediately juxtaposed with the MTOC to the target cell synapse (juxtaposed) (Fig. 3*C*). In the absence of target cells, most NK cells displayed dispersed granules. On conjugation with K562 cells, about 50% of NK cells from healthy donors had perforin granules polarized or immediately juxtaposed to the target cell synapse. A similar pattern of perforin granule polarization was observed in NK cells from the ORAI1-deficient patient (Fig. 3*D*). The degree of perforin polarization toward K562 cells was similar to what has been reported previously (26). These results indicate that initial signals for adhesion and granule polarization are independent of ORAI1-mediated Ca^{2+} influx in NK cells.

Severely Impaired NK Cell Degranulation in the Absence of ORAI1 or STIM1. Degranulation of cytotoxic lymphocytes can be quantified by determining the surface expression of CD107a following stimulation (27). K562 cells and P815 cells with anti-CD16 mAb induced strong degranulation of control but not of ORAI1-deficient or STIM1-deficient NK cells (Fig. 4 *A* and *B* and Fig. S8). Similar results were obtained when degranulation was induced through engagement of defined NK cell activation receptors by ligands expressed by S2-cell transfectants (Fig. S9). Furthermore, target cell-induced degranulation of CD56^{dim} NK cells was significantly impaired after pretreatment of cells with the inhibitor DPB162-AE and following coincubation with K562 cells or anti–CD16-coated P815 cells (Fig. 4 *C* and *D*). A similar degranulation defect was observed in DPB162-AE–pretreated CD8$^+$ CD62L$^-$ effector T cells coincubated with P815 cells plus anti-CD3. At a concentration of 100 μM, 2-APB reduced K562 cell-mediated CD56^{dim} NK cell degranulation by 87%, but did not affect inside-out signals for activation of LFA-1. Taken together, these results demonstrated that cytotoxic lymphocyte degranulation induced by a variety of stimuli required SOCE mediated by STIM1 and ORAI1.

Impaired Cytokine Production of ORAI1-Deficient NK Cells Is Dependent on the Activating Stimulus. Because ORAI1 plays a key role in cytokine production by helper T cells, we also studied the expression of chemokines and cytokines in CD56^{dim} NK cells in response to stimulation by K562 cells or P815 cells plus anti-CD16 mAb. Macrophage inflammatory protein-1β (MIP-1β) was expressed in 80–87% of CD56^{dim} NK cells from healthy donors and in 26–41% of CD56^{dim} NK cells from the ORAI1-deficient patient (Fig. 5 *A* and *B*), indicating a partial dependence of MIP-1β production on ORAI1. The production of IFN-γ and TNF-α in response to the same stimuli was fully dependent on ORAI1 (Fig. 5 *A* and *B*). By contrast, stimulation by combinations of IL-12, IL-15, and IL-18 was able to elicit normal production of MIP-1β and IFN-γ in human ORAI1-deficient CD56^{dim} NK cells (Fig. 5*C*). These data suggest that target cell recognition by NK cells induces ORAI1-dependent cytokine production, whereas ORAI1 is not required for production of cytokines in response to exogenous cytokine stimuli.

Discussion

This study identifies SOCE mediated by STIM1 and ORAI1 as the key mechanism of extracellular Ca^{2+} influx required for granule exocytosis and cytotoxicity in human cytotoxic lymphocytes. Moreover, a role for ORAI1 in cytokine production by NK cells specifically in response to target cell ligands is documented.

NK cells obtained from an ORAI1-deficient patient and a STIM1-deficient patient had severely impaired natural cytotoxicity. The former patient carries a homozygous mutation in *ORAI1,* leading to a R91W single amino acid substitution. It has previously been shown that this mutation abolishes CRAC channel function in human T cells (13). Our results show that stimulation of NK cells from this patient failed to induce a sustained rise in the concentration of intracellular free calcium. Because of the severe clinical condition of the latter patient, the functional consequences of the *STIM1* mutation could not be fully characterized; however, Ca^{2+} influx in T cells was severely impaired. The defect in Ca^{2+} influx is of similar severity in freshly isolated ORAI1-deficient NK cells as in T-cell lines, suggesting that SOCE in human NK cells is mediated predominantly by ORAI1 and not by other Ca^{2+} channels. Previous studies with T cells from the same patient have established that ORAI1 is required for activation of the transcription factor NFAT; for mitogen-mediated T-cell proliferation; and for the production of cytokines, such as IL-2, IL-4, IFN-γ, and TNF-α, in response to cross-linking of the T-cell receptor or stimulation with phorbol 12-myristate 13-acetate (PMA) and ionomycin (13, 18, 28). Altogether, these results have clearly demonstrated an important role for ORAI1 in T-cell activation. Whether SOCE

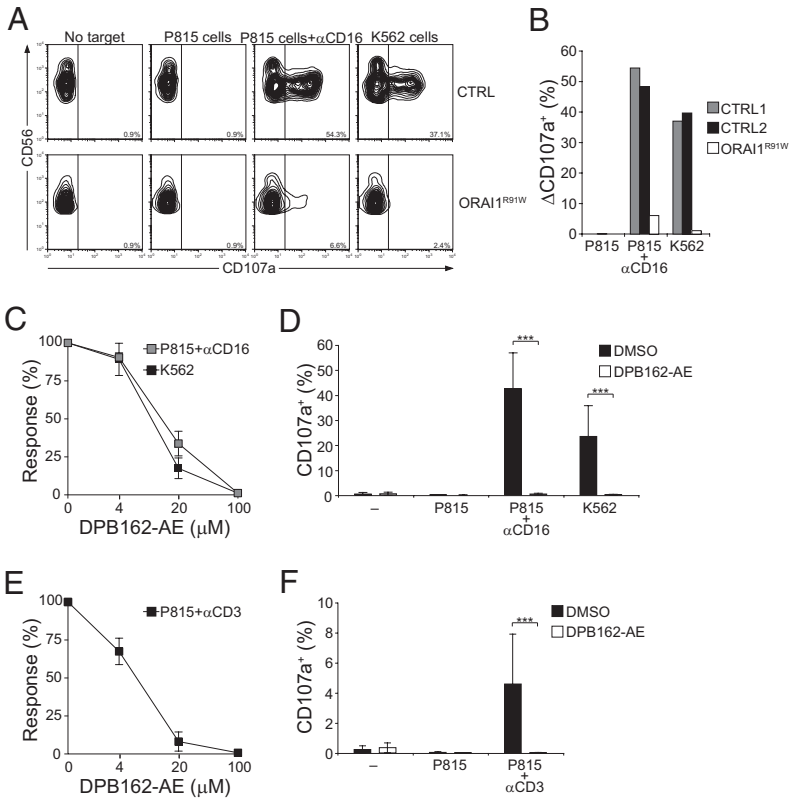

Fig. 4. Cytotoxic lymphocyte degranulation requires ORAI1. (*A* and *B*) PBMCs from the ORAI1-deficient patient (ORAI1^{R91W}) or healthy donors (CTRL) were stimulated with target cells as indicated for 2 h at 37 °C and thereafter stained with fluorochrome-conjugated lineage markers and anti-CD107 anti-mAbs. Lymphocytes were gated on forward scatter/side scatter characteristics. CTRL, control. (*A*) CD56 vs. CD107a expression is plotted on CD3$^-$CD56$^+$ NK cells. (*B*) Percent increase of CD107a$^+$CD56^{dim} NK cells after incubation with target cells relative to CD107a$^+$CD56^{dim} NK cells without target cells (ΔCD107a$^+$) is presented. One representative experiment of four is shown. (*C*–*F*) PBMCs from healthy donors were preincubated with DPB162-AE, stimulated with target cells as indicated for 2 h at 37 °C, stained with fluorochrome-conjugated lineage markers and anti-CD107 anti-mAbs, and evaluated for surface expression of CD107a on CD56^{dim} NK cells. The graph depicts the percent response of CD107a surface expression on CD56^{dim} NK cells (*C*) and CD8$^+$CD62L$^-$ T cells (*E*) at varying DPB162-AE concentrations relative to that with vehicle only. The plot depicts the percentage of CD107a$^+$CD56^{dim} NK cells (*D*) and CD107a$^+$CD8$^+$CD62L$^-$ T cells (*F*) after incubation with or without 100 μM DPB162-AE. Values with error bars represent mean ± SD of four (*C* and *E*) or eight (*D* and *F*) donors.

mediated by ORAI1 and STIM1 facilitates lymphocyte cytotoxicity has not been assessed thus far, however (2, 10).

In studies of T-cell lines, Ca^{2+} influx has been implicated in MTOC polarization (29, 30). We found no impairment of granule and MTOC polarization in ORAI1-deficient NK cells on target cell conjugation. This is in line with recent evidence from murine helper T cells in which extracellular Ca^{2+} was not required for MTOC polarization (31). Moreover, LFA-1 engagement is sufficient to induce polarization of perforin granules in freshly isolated NK cells, without detectable intracellular mobilization of Ca^{2+} (32). Rather, we found a clear defect in the exocytosis of lytic granules by ORAI1-deficient NK cells following engagement of CD16 or coengagement of 2B4 and NKG2D receptors. Of note, these stimuli were able to induce inside-out signals for LFA-1 activation in the absence of ORAI1, revealing a specific requirement for ORAI1-mediated Ca^{2+} influx for degranulation and cytotoxicity and not a general defect in NK cell activating signaling per se. Importantly, the target cell-induced degranulation defect could also be observed in NK cells from the STIM1-deficient patient, providing independent evidence for the key role of SOCE in this process.

In an additional set of experiments, we could show that pretreatment of cytotoxic lymphocytes with the ORAI1 inhibitor DPB162-AE inhibits granule exocytosis and cytotoxicity in a dose-dependent fashion. DPB162-AE is a recently described 2-APB analog that inhibits endogenous SOCE (21). Because the compound inhibits store depletion-mediated STIM1 clustering as well as heterologously expressed CRAC current, it was suggested that its effect on SOCE is mediated by inhibiting STIM1 aggregation and transactivation of ORAI1. These inhibitors may also inhibit related CRAC channels, such as ORAI2 and ORAI3. DPB162-AE inhibited SOCE in human NK cells, and pretreatment of NK cells with the inhibitor impaired degranulation, cytotoxicity, and cytokine production but did not impair inside-out signals for LFA-1 activation. This not only mirrors the findings obtained with the ORAI1-deficient patient's cells but illustrates that other ORAI1-independent functions are preserved in DPB162-AE–treated NK cells, arguing against a general nonspecific effect on signaling for NK cell activation. Importantly, use of the inhibitor also allowed investigations of CTLs. Because NK cells share several mechanisms for target cell elimination with CTLs (33, 34) and CRAC channel currents have been implicated in CTL exocytosis (9), it was not unexpected that pharmacological inhibition of SOCE blocked CTL-mediated granule exocytosis and reduced CTL cytotoxicity. These latter observations require confirmation in CTLs from ORAI1- or STIM1-deficient patients, but a more general role for ORAI1 in granule exocytosis by immune cells is also supported by the finding that *Orai1*-deficient mouse mast cells display defective degranulation (35). Finally, in an ongoing study, we have found that NK cells from knock-in mice homozygous for a R93W amino acid substitution in Orai1 that is equivalent to the R91W mutation found in ORAI1-deficient patients are also deficient in target-cell induced degranulation and cytokine production (36).

Taken together, our observations provide important insights into the mechanisms of Ca^{2+} influx in cytotoxic lymphocytes and its role in lytic granule exocytosis and cytotoxicity. We identified ORAI1 as a key Ca^{2+} channel mediating SOCE in NK cells and showed that SOCE mediated by STIM1 and ORAI1 is essential for NK cell function. With respect to understanding cytotoxic lymphocyte exocytosis, analogies between the function of the neurological and immunological synapses are increasingly apparent, including a requirement for high cytosolic Ca^{2+} concentration in triggering exocytosis (37). A number of proteins with a high degree of homology to mediators of vesicle fusion and exocytosis in neurons have been implicated in lymphocyte cytotoxicity. Some of these proteins, such as Munc13-4 and synaptotagmin VII, are expressed in immune cells and contain Ca^{2+}-binding domains (38, 39). Munc13-4 is required for cytotoxic lymphocyte exocytosis, and Munc13-4 deficiency causes immunodeficiency in humans and mice (40, 41). Moreover, synaptotagmin VII-deficient mice display impaired target cell lysis (42). These proteins may therefore act as sensors of Ca^{2+} influx for lytic granule exocytosis.

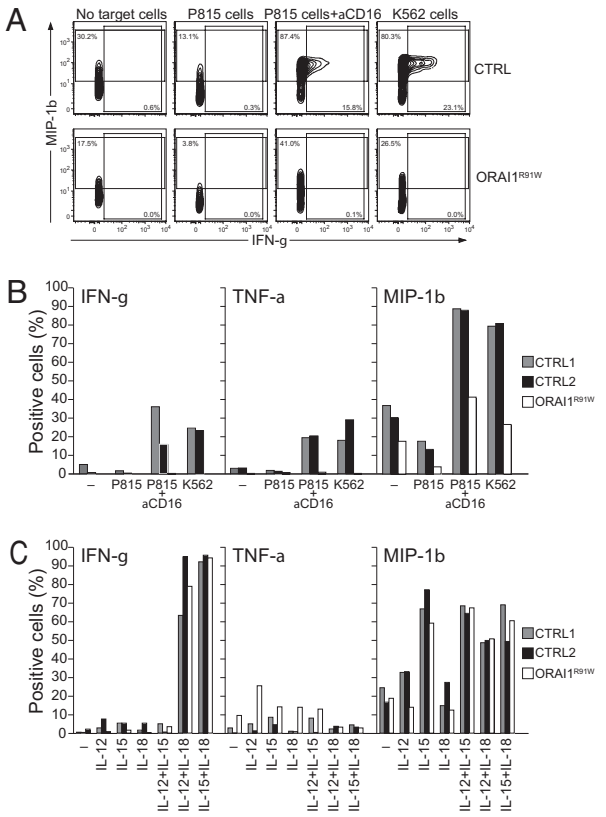

Fig. 5. Defective chemokine and cytokine production by ORAI1-deficient NK cells on engagement of activation receptors. PBMCs were mixed with target cells (*A* and *B*) or cytokines (*C*) as indicated. Cells were stimulated for 6 h (*A* and *B*) or 24 h (*C*) at 37 °C, followed by surface staining with fluorochrome-conjugated lineage marker mAbs and intracellular staining with fluorochrome-conjugated anti–IFN-γ, anti–MIP-1β, and anti–TNF-α mAbs. (*A*) Lymphocytes were gated on forward scatter/side scatter characteristics. CD56 vs. CD107a expression is shown for $CD3^{-}CD56^{dim}$ NK cells. (*B* and *C*) Percentage of $CD56^{dim}$ NK cells expressing the indicated chemokines and cytokines after incubation with target cells is presented. One representative experiment of three is shown. CTRL, control; $ORAI1^{R91W}$, ORAI1-deficient.

A role of ORAI1 in T-cell cytokine production in response to stimulation with PMA and ionomycin or with anti-CD3 and anti-CD28 is well documented (18, 28, 35, 43, 44). Our data, obtained with ORAI1-deficient and inhibitor-treated NK cells, indicate a similar requirement of ORAI1 for expression of IFN-γ and TNF-α induced by engagement of activating receptors on NK cells. These results are consistent with observations that CD16-mediated signals in NK cells induce nuclear translocation of NFAT (18, 28, 45). Expression of the chemokine MIP-1β was only partially impaired in ORAI1-deficient NK cells. Similar data have been reported for ORAI1-deficient T-cell lines (28). Thus, chemokine production can be disassociated from SOCE, in line with findings demonstrating that engagement of NK cell receptors not capable of inducing signals for degranulation still could mediate chemokine secretion for recruitment of other immune cells (46). Notably, no defect in production of IFN-γ, TNF-α, or MIP-1β was evident after NK cell stimulation with combinations of exogenous cytokines, such as IL-12, IL-15, and IL-18. Thus, ORAI1 is specifically required for NK cell cytokine production induced by receptors for target cell recognition.

The findings described in our study provide evidence for a role of ORAI1-mediated Ca^{2+} influx in cytotoxic lymphocyte function and have several important implications. First, we show that ORAI1 and STIM1 are required for NK cell function. NK cells from patients with genetic defects in CRAC channel function unequivocally show that ORAI1 and STIM1 are required for Ca^{2+} influx in NK cells and for their cytolytic function. Second, specific ORAI1 inhibitors may therefore pave the way for therapeutical strategies targeting cytotoxic lymphocyte-mediated immunopathology (e.g., in situations of perforin-mediated autoimmunity and allograft rejection). Third, our findings show that about 10–15% of normal T cells and 5% of normal B cells in an ORAI1-deficient host are sufficient for protective immunity to most pathogens. This low level of mixed chimerism has supported normal T-cell proliferation and IgG antibody responses to several vaccinations as well as control of a variety of infections. Finally, our data identify a simple diagnostic tool to screen for Ca^{2+} channel defects in patients with immunodeficiency. Quantification of NK cell degranulation in response to target cell stimulation has proven to be valuable in the differential diagnosis of human defects of cellular cytotoxicity, requires small amounts of peripheral blood mononuclear cells (PBMCs), and is robust even during severe infections (47, 48).

Methods

Patients. Brief case reports of the patients are presented in *SI Methods*. Informed consent was obtained for the performed studies according to the regulations of the Ethics Committee of the University of Freiburg.

Cells and Antibodies. PBMCs were isolated by Ficoll density gradient centrifugation (PAN-Biotec). NK cells were isolated by negative immunomagnetic selection (Miltenyi Biotec). Purity of the isolated $CD3^{-}CD56^{+}$ NK cells was >95%. The human erythroleukemia cell line K562, the mouse mastocytoma cell line P815, and the mouse leukemia cell line L1210 (all from the American Type Culture Collection) were used as target cells. Antibodies are listed in *SI Methods*.

Chimerism Analysis. For chimerism analysis, DNA was extracted from $CD3^{-}CD56^{+}$ NK cells, $CD19^{+}$ B cells, and $CD3^{+}$ T cells sorted on a Mo Flo cell sorter (Beckman Coulter) to >95% purity. STR analysis was performed with an AmpF/STR Identifier PCR amplification kit (Applied Biosystems).

Measurement of Intracellular Calcium. Intracellular Ca^{2+} flux was investigated by flow cytometry using cells loaded with indo-1-AM (Invitrogen), a Ca^{2+}-sensitive fluorescent dye (49). Freshly isolated NK cells were preincubated with anti-CD16 mAb for 30 min at 4 °C, loaded with 5 μM indo-1 in Iscove's modified Dulbecco's medium and 1% FBS for 45 min at 37 °C, washed once, and adjusted to a cell concentration of 1×10^6 cells/mL in Ca^{2+}-free PBS supplemented with 1% FBS. Cells were analyzed on an LSR II flow cytometer (BD Bioscience) using FACS Diva Software (version 6.1.2; BD Bioscience).

Cytotoxicity Assays. The cytolytic activity of freshly isolated NK cells was measured by standard 4-h ^{51}Cr release assays. K562, L1210, or P815 target cells were labeled with ^{51}Cr and either used directly (K562 cells) or after incubation for 15 min at room temperature with 10 μg/mL anti-CD16 (L1210 cells). Target cells were incubated with freshly isolated human NK cells at different effector/target cell ratios. Supernatants were measured on a γ-counter (Packard–Cobra).

Inside-Out Signaling Assay. To evaluate LFA-1 conformational changes, 2×10^5 PBMCs were mixed with 2×10^5 target cells in 100 μL of complete medium as previously described (25). The cells were spun down for 1 min at $20 \times g$ and incubated for 5 min at 37 °C. In experiments with pharmacological inhibitors of ORAI1, the cells were incubated for 2 h at 37 °C to assess for surface CD107a simultaneously. Following stimulation, the cells were stained with biotinylated LFA-1 conformation-specific mAbs in ice-cold PBS supplemented with 2% (vol/vol) FBS for 45 min. Cells were washed and stained with fluorochrome-conjugated anti-CD3 and anti-CD56, in addition to fluorochrome-conjugated streptavidin. Finally, cells were resuspended in PBS with 2% (vol/vol) FBS and analyzed by flow cytometry. Data were analyzed with FlowJo 8.6 software (Treestar, Inc.).

Granule Polarization Assay. NK cells were mixed at a 1:1 ratio with K562 cells and incubated on microscope slides for 20 min at 37 °C. Cells were fixed in 4% (vol/vol) paraformaldehyde (Sigma–Aldrich), permeabilized with 0.05% saponin, blocked with 10% (vol/vol) FBS and 1% BSA, and then labeled with fluorochrome-conjugated phalloidin and antiperforin as well as anti–α-tubulin mAbs. Conjugates were imaged with an inverted spinning disk con-

focal microscope (Andor) and then scored blinded for the degree of polarization of perforin, MTOC, and F-actin.

Degranulation Assays. NK cell degranulation was assessed as previously described (48). Briefly, 2×10^5 PBMCs were mixed with 2×10^5 target cells in 200 μL of complete medium. Cells were mixed, spun down for 3 min at $20 \times g$, and incubated for 2 h at 37 °C. Thereafter, the cells were spun down; stained with fluorochrome-conjugated mAbs against CD3, CD56, and CD107a in PBS supplemented with 2% (vol/vol) FBS and 2 mM EDTA for 45 min on ice; washed; resuspended in PBS supplemented with 2% (vol/vol) FBS and 2 mM EDTA; and analyzed by flow cytometry.

Intracellular Cytokine Staining. For stimulation with target cells, 2×10^5 PBMCs were added to 2×10^5 target cells in 200 μL of complete medium as previously described (46). Briefly, after incubation of the cells for 1 h at 37 °C, Brefeldin A (GolgiPlug; BD Bioscience) was added, followed by an additional 5 h of incubation. In some experiments, cells were stimulated with 10 ng/mL IL-12 (Peprotech), 100 ng/mL IL-15 (Peprotech), and/or 100 ng/mL IL-18 (R&D Systems). For stimulation with exogenous cytokines, cells were stimulated for 19 h at 37 °C before addition of Brefeldin A and an additional 5 h of incubation. The cells were analyzed on a CyAn ADP LX nine-color flow cytometer (Dako).

Statistical Analysis. Statistical significance was evaluated with a nonparametric Mann–Whitney test using Graphpad Prism software.

ACKNOWLEDGMENTS. We acknowledge the technical assistance of A. Ott. This work was supported by Bundesministerium für Bildung und Forschung Grant 01 EO 0803 (to S.E.), Deutsche Forschungsgemeinschaft Grants SFB620 TP A4 (to S.E.) and SFB620 TP B6 (to W.W.S.), the Deutsche Forschungsgemeinschaft Emmy Noether program (T.B. and W.W.S.), the Swedish Research Council, the Society for Medical Research, the Mary Beve's Foundation, Clas Groschinsky's Memorial Fund, the Shizu Matsumaras Donation, the Karolinska Institute Research Foundation (Y.T.B.), the Swedish Research Council (C.F.), and National Institutes of Health Grant AI066128 (to S. Feske).

1. Dustin ML, Long EO (2010) Cytotoxic immunological synapses. *Immunol Rev* 235: 24–34.
2. de Saint Basile G, Ménasché G, Fischer A (2010) Molecular mechanisms of biogenesis and exocytosis of cytotoxic granules. *Nat Rev Immunol* 10:568–579.
3. Kuhn JR, Poenie M (2002) Dynamic polarization of the microtubule cytoskeleton during CTL-mediated killing. *Immunity* 16:111–121.
4. Griffiths GM, Tsun A, Stinchcombe JC (2010) The immunological synapse: A focal point for endocytosis and exocytosis. *J Cell Biol* 189:399–406.
5. Pipkin ME, Lieberman J (2007) Delivering the kiss of death: Progress on understanding how perforin works. *Curr Opin Immunol* 19:301–308.
6. Lancki DW, Weiss A, Fitch FW (1987) Requirements for triggering of lysis by cytolytic T lymphocyte clones. *J Immunol* 138:3646–3653.
7. Takayama H, Sitkovsky MV (1987) Antigen receptor-regulated exocytosis in cytotoxic T lymphocytes. *J Exp Med* 166:725–743.
8. Leibson PJ, Midthun DE, Windebank KP, Abraham RT (1990) Transmembrane signaling during natural killer cell-mediated cytotoxicity. Regulation by protein kinase C activation. *J Immunol* 145:1498–1504.
9. Lyubchenko TA, Wurth GA, Zweifach A (2001) Role of calcium influx in cytotoxic T lymphocyte lytic granule exocytosis during target cell killing. *Immunity* 15:847–859.
10. Pores-Fernando AT, Zweifach A (2009) Calcium influx and signaling in cytotoxic T-lymphocyte lytic granule exocytosis. *Immunol Rev* 231:160–173.
11. Liou J, et al. (2005) STIM is a Ca2+ sensor essential for Ca2+-store-depletion-triggered Ca2+ influx. *Curr Biol* 15:1235–1241.
12. Roos J, et al. (2005) STIM1, an essential and conserved component of store-operated Ca2+ channel function. *J Cell Biol* 169:435–445.
13. Feske S, et al. (2006) A mutation in Orai1 causes immune deficiency by abrogating CRAC channel function. *Nature* 441:179–185.
14. Vig M, et al. (2006) CRACM1 is a plasma membrane protein essential for store-operated Ca2+ entry. *Science* 312:1220–1223.
15. Hogan PG, Lewis RS, Rao A (2010) Molecular basis of calcium signaling in lymphocytes: STIM and ORAI. *Annu Rev Immunol* 28:491–533.
16. Feske S (2009) ORAI1 and STIM1 deficiency in human and mice: Roles of store-operated Ca2+ entry in the immune system and beyond. *Immunol Rev* 231:189–209.
17. Picard C, et al. (2009) STIM1 mutation associated with a syndrome of immunodeficiency and autoimmunity. *N Engl J Med* 360:1971–1980.
18. Feske S, et al. (1996) Severe combined immunodeficiency due to defective binding of the nuclear factor of activated T cells in T lymphocytes of two male siblings. *Eur J Immunol* 26:2119–2126.
19. Schlesier M, et al. (1993) Primary severe immunodeficiency due to impaired signal transduction in T cells. *Immunodeficiency* 4:133–136.
20. Cahalan MD, Chandy KG (2009) The functional network of ion channels in T lymphocytes. *Immunol Rev* 231:59–87.
21. Goto J, et al. (2010) Two novel 2-aminoethyl diphenylborinate (2-APB) analogues differentially activate and inhibit store-operated Ca(2+) entry via STIM proteins. *Cell Calcium* 47:1–10.
22. Bryceson YT, March ME, Ljunggren HG, Long EO (2006) Activation, coactivation, and costimulation of resting human natural killer cells. *Immunol Rev* 214:73–91.
23. Orange JS (2008) Formation and function of the lytic NK-cell immunological synapse. *Nat Rev Immunol* 8:713–725.
24. Beals CR, Edwards AC, Gottschalk RJ, Kuijpers TW, Staunton DE (2001) CD18 activation epitopes induced by leukocyte activation. *J Immunol* 167:6113–6122.
25. Bryceson YT, Ljunggren HG, Long EO (2009) Minimal requirement for induction of natural cytotoxicity and intersection of activation signals by inhibitory receptors. *Blood* 114:2657–2666.
26. Orange JS, et al. (2003) The mature activating natural killer cell immunologic synapse is formed in distinct stages. *Proc Natl Acad Sci USA* 100:14151–14156.
27. Betts MR, et al. (2003) Sensitive and viable identification of antigen-specific CD8+ T cells by a flow cytometric assay for degranulation. *J Immunol Methods* 281:65–78.
28. Feske S, Draeger R, Peter HH, Eichmann K, Rao A (2000) The duration of nuclear residence of NFAT determines the pattern of cytokine expression in human SCID T cells. *J Immunol* 165:297–305.
29. Kupfer A, Swain SL, Singer SJ (1987) The specific direct interaction of helper T cells and antigen-presenting B cells. II. Reorientation of the microtubule organizing center and reorganization of the membrane-associated cytoskeleton inside the bound helper T cells. *J Exp Med* 165:1565–1580.
30. Kuhné MR, et al. (2003) Linker for activation of T cells, zeta-associated protein-70, and Src homology 2 domain-containing leukocyte protein-76 are required for TCR-induced microtubule-organizing center polarization. *J Immunol* 171:860–866.
31. Quann EJ, Merino E, Furuta T, Huse M (2009) Localized diacylglycerol drives the polarization of the microtubule-organizing center in T cells. *Nat Immunol* 10:627–635.
32. Bryceson YT, March ME, Barber DF, Ljunggren HG, Long EO (2005) Cytolytic granule polarization and degranulation controlled by different receptors in resting NK cells. *J Exp Med* 202:1001–1012.
33. Fischer A, Latour S, de Saint Basile G (2007) Genetic defects affecting lymphocyte cytotoxicity. *Curr Opin Immunol* 19:348–353.
34. Stinchcombe JC, Griffiths GM (2007) Secretory mechanisms in cell-mediated cytotoxicity. *Annu Rev Cell Dev Biol* 23:495–517.
35. Vig M, et al. (2008) Defective mast cell effector functions in mice lacking the CRACM1 pore subunit of store-operated calcium release-activated calcium channels. *Nat Immunol* 9:89–96.
36. Bergmeier W, et al. (2009) R93W mutation in Orai1 causes impaired calcium influx in platelets. *Blood* 113:675–678.
37. Dustin ML, Colman DR (2002) Neural and immunological synaptic relations. *Science* 298:785–789.
38. Li C, et al. (1995) Ca(2+)-dependent and -independent activities of neural and non-neural synaptotagmins. *Nature* 375:594–599.
39. Koch H, Hofmann K, Brose N (2000) Definition of Munc13-homology-domains and characterization of a novel ubiquitously expressed Munc13 isoform. *Biochem J* 349: 247–253.
40. Feldmann J, et al. (2003) Munc13-4 is essential for cytolytic granules fusion and is mutated in a form of familial hemophagocytic lymphohistiocytosis (FHL3). *Cell* 115: 461–473.
41. Crozat K, et al. (2007) Jinx, an MCMV susceptibility phenotype caused by disruption of Unc13d: A mouse model of type 3 familial hemophagocytic lymphohistiocytosis. *J Exp Med* 204:853–863.
42. Fowler KT, Andrews NW, Huleatt JW (2007) Expression and function of synaptotagmin VII in CTLs. *J Immunol* 178:1498–1504.
43. Gwack Y, et al. (2008) Hair loss and defective T- and B-cell function in mice lacking ORAI1. *Mol Cell Biol* 28:5209–5222.
44. Feske S, Giltnane J, Dolmetsch R, Staudt LM, Rao A (2001) Gene regulation mediated by calcium signals in T lymphocytes. *Nat Immunol* 2:316–324.
45. Aramburu J, Azzoni L, Rao A, Perussia B (1995) Activation and expression of the nuclear factors of activated T cells, NFATp and NFATc, in human natural killer cells: Regulation upon CD16 ligand binding. *J Exp Med* 182:801–810.
46. Fauriat C, Long EO, Ljunggren HG, Bryceson YT (2010) Regulation of human NK-cell cytokine and chemokine production by target cell recognition. *Blood* 115:2167–2176.
47. Marcenaro S, et al. (2006) Analysis of natural killer-cell function in familial hemophagocytic lymphohistiocytosis (FHL): Defective CD107a surface expression heralds Munc13-4 defect and discriminates between genetic subtypes of the disease. *Blood* 108:2316–2323.
48. Bryceson YT, et al. (2007) Defective cytotoxic lymphocyte degranulation in syntaxin-11 deficient familial hemophagocytic lymphohistiocytosis 4 (FHL4) patients. *Blood* 110:1906–1915.
49. Minguet S, Swamy M, Alarcón B, Luescher IF, Schamel WW (2007) Full activation of the T cell receptor requires both clustering and conformational changes at CD3. *Immunity* 26:43–54.